Sulfur-annulated Perylenediimide as Interfacial Materials Enabling Inverted Perovskite Solar Cells with over 20% Efficiency and High Fill Factor Exceeding 83%

Fei Wu,[‡a] Zhenghui Luo,[‡b,c] Linna Zhu,[*a] Chao Chen,[d] Huiqiang Lu,[a] Zhanxiang Chen[c], Jiang Tang[d] and Chuluo Yang[*b,c]

[a]*Chongqing Key Laboratory for Advanced Materials and Technologies of Clean Energy, Faculty of Materials & Energy, Southwest University, Chongqing 400715, P.R. China.*

[b]*College of Materials Science and Engineering, Shenzhen University, Shenzhen, 518060, P.R. China*

[c]*Hubei Key Lab on Organic and Polymeric Optoelectronic Materials, Department of Chemistry, Wuhan University. Wuhan 430072, P. R. China.*

[d]*Wuhan National Laboratory for Optoelectronics (WNLO), Huazhong University of Science and Technology, 1037 Luoyu Road, Wuhan 430074, Hubei, PR China.*

Experimental section

Materials and instruments

Unless otherwisely stated, all starting materials were purchased from commercial suppliers (Sigma-Aldrich and Energy Chemical) and used without further purification, including P3CT (Rieke Metals), PbI_2 (p-OLED, >99.99%), $PbCl_2$ (p-OLED, >99.99%), MAI (p-OLED, ≥99.5%), $PC_{61}BM$ (p-OLED, ≥99%), C_{60} (p-OLED), BCP (p-OLED), DMF (Sigma-Aldrich, 99.8%), DMSO (Sigma-Aldrich, 99.8%) and CB (Sigma-Aldrich, 99.8%). UV-vis-NIR absorption spectra were recorded on a Shimadzu UV-2501 recording spectrophotometer. Cyclic voltammetry (CV) measurements were carried out on a CHI voltammetric analyzer at room temperature. Tetrabutylammonium hexafluorophosphate (*n*-Bu_4NPF_6, 0.1 M) was used as the supporting electrolyte. The conventional

three-electrode configuration consists of a platinum working electrode with a 2 mm diameter, a platinum wire counter electrode, and an Ag/AgCl wire reference electrode. Cyclic voltammograms were obtained at a scan rate of 100 mV/s. Fluorescence spectra were measured on a Hitachi F-4600 FL Spectrophotometer. The PL lifetimes were measured by a single photon counting spectrometer from Edinburgh Instruments (FLS920) with a Picosecond Pulsed UV-LASTER (LASTER377) as the excitation source. Field-emission SEM (FE-SEM) image was taken on JSM-7800F. AFM images were collected in air on a Bruker AFM using a tapping mode. The capacitance-voltage (C-V) profiling data was measured using Keithley 4200. C-V measurements were performed at room temperature in an electromagnetic shielding box at a frequency of 100 kHz and AC amplitude of 30 mV. DC bias voltage was changed from -1 V to 1.1 V. For transient photovoltage/photocurrent decay measurements, a 532 nm pulse helium-neon laser modulated by a function generator with pulsed signal (frequency 1 kHz) was used. The two electrodes of solar cell were connected to the signal sampling channels of Agilent oscilloscope (Agilent DSOS054A), and the decay signal was collected with a rising edge trigger.

Synthesis and Characterizations

All solvents and reagents were used as received from commercial sources and used without further purification unless otherwise specified. ^{1}H NMR (300 MHz) and ^{13}C NMR (75 MHz) spectra were measured on a MERCURYVX300 spectrometers. MALDI-TOF MS spectra were performed on a AB 5800 instrument, using CHCA as a matrix. Compound PDI-S-Br was synthesized according to literature.[1]

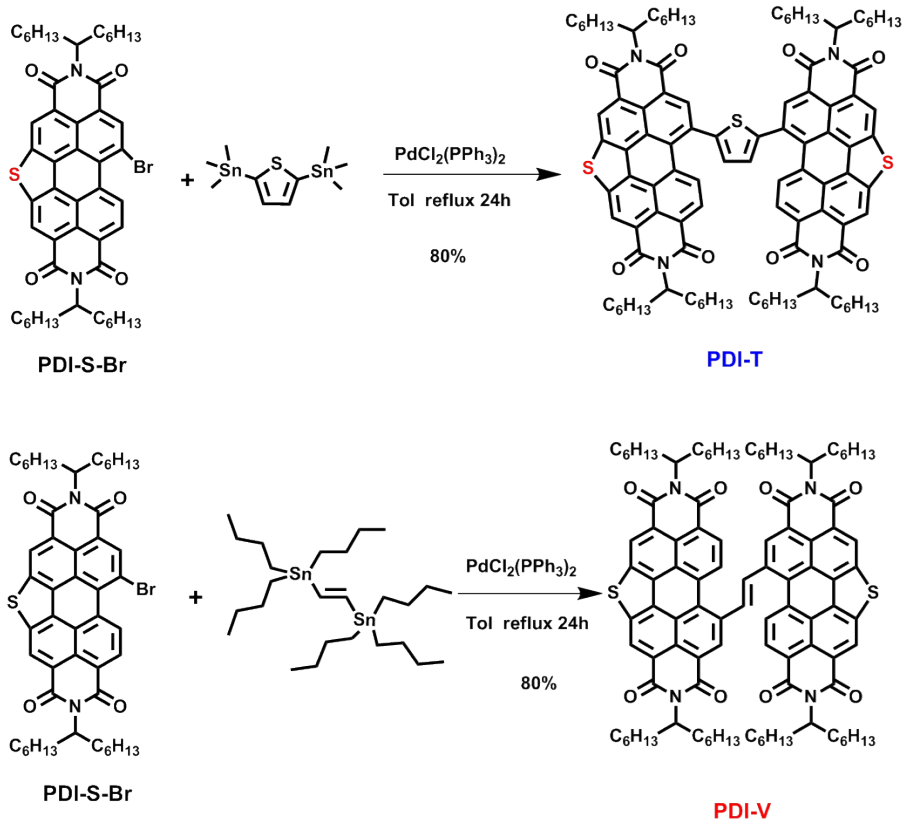

Scheme S1. Synthetic routes for PDI-T and PDI-V.

PDI-T: A mixture of 2,5-bis(trimethylstannyl)thiophene (68 mg, 0.1649 mmol), PDI-S-Br (313 mg, 0.3632 mmol), and $PdCl_2(PPh_3)_2$ (20 mg) in anhydrous toluene (10 mL) in a Schlenk tube was subjected to three cycles of evacuation and admission of nitrogen and subsequently stirred at 110 °C for 24 h. The reaction mixture was allowed to cool to room temperature and the solvent was removed under vacuum. The crude product was purified by silica gel column chromatography with hexane/dichloromethane (1:1) as an eluent to give the target product PDI-T as a red solid with a yield of 80%. ^{1}H NMR ($CDCl_3$, 300 MHz): δ [ppm]: 9.50-9.35 (m, 4H), 9.18-9.03 (m, 2H), 8.80 (s, 4H), 7.57 (s, 2H), 5.40-5.20 (m, 4H), 2.45-2.20 (m, 8H), 2.00-1.75 (m, 8H), 1.54-1.09 (m, 64H), 0.88-0.76 (m, 24H). ^{13}C NMR (100 MHz, CDCl3): δ [ppm]: 165.03, 163.97, 163.37, 146.06, 143.71, 141.25, 138.37, 138.14, 137.88, 133.48, 132.34, 131.80, 128.11, 127.78, 126.21, 124.55, 124.24, 122.61, 121.29, 54.97, 53.37, 32.35, 31.68, 29.73, 29.19, 27.02, 26.93, 26.86, 23.94, 22.62, 22.52,

14.08, 14.01. MS (MALDI-TOF): calcd for ($C_{104}H_{120}N_4O_8S_3$), 1648.8; found, 1648.9. Elemental anal. calcd for $C_{104}H_{120}N_4O_8S_3$: C, 75.69%; H, 7.33%; N 3.39%. Found: C, 75.42%; H, 7.30%; N 3.33%.

PDI-V: A mixture of trans-1,2-Bis(tributylstannyl)ethene (100 mg, 0.1649 mmol), PDI-S-Br (313 mg, 0.3632 mmol), and $PdCl_2(PPh_3)_2$ (20 mg) in anhydrous toluene (10 mL) in a Schlenk tube was subjected to three cycles of evacuation and admission of nitrogen and subsequently stirred at 110 °C for 24 h. The reaction mixture was allowed to cool to room temperature and the solvent was removed under vacuum. The crude product was purified by silica gel column chromatography with hexane/dichloromethane (2:3) as an eluent to give the target product PDI-V as a red solid with a yield of 80%. ^{1}H NMR ($CDCl_3$, 300 MHz): δ [ppm]: 9.40-9.00 (m, 6H), 8.70 (s, 2H), 8.47 (s, 2H), 5.40-5.00 (m, 4H), 2.40-2.00 (m, 8H), 2.00-1.80 (m, 8H), 1.50-1.00 (m, 64H), 0.88-0.76 (m, 24H). ^{13}C NMR (100 MHz, CDCl3): δ [ppm]: 165.44, 164.33, 1 163.69, 147.64, 146.16, 141.47, 140.64, 139.86, 137.28, 134.60, 133.89, 131.02, 129.92, 128.95, 128.12, 126.48, 126.06, 125.91, 125.81, 125.72, 122.26, 121.94, 54.93, 54.74, 32.27, 31.66, 31.56, 29.14, 26.85, 22.47, 22.38, 13.90, 13.83. MS (MALDI-TOF): calcd for ($C_{102}H_{120}N_4O_8S_2$), 1592.9; found, 1592.91. Elemental anal. calcd for $C_{102}H_{120}N_4O_8S_2$: C, 76.85%; H, 7.59%; N 3.51%. Found: C, 76.78%; H, 7.69%; N 3.39%.

Device fabrication

The devices fabrication procedures can be referred to our previous work. The indium tin oxide (ITO) glass substrates were sequentially washed by sonication using detergent, deionized water, ethanol and acetone. The hole transporting layer P3CT-Na was formed on ITO substrates by spin coating at

4000 rpm for 60 s followed by annealing at 140°C for 30 min.[2] Then the samples were transferred into a N_2-filled glovebox. A perovskite precursor solution (1.26 M PbI_2, 0.14 M $PbCl_2$ and 1.40 M MAI in DMF:DMSO mixed solution with a v/v of 4:1) was spin-coated in a two-step program at 400 and 5000 rpm for 3 and 30 s, respectively. During the second step, 200 μL of chlorobenzene was dropped on the spinning substrate at 10 s after the start-up. Next, the as-spun perovskite layer was annealed on a hot plate at 60 °C for 1 min and at 85 °C for 25 min to drive off solvent and form the perovskite phase. Then PDI-T/PDI-V in chlorobenzene were spin-coated onto the perovskite layer. To fabricate ITO/P3CT-Na/Perovskite/ PDI-T or PDI-V /C_{60}/BCP/Ag device, C_{60} (40 nm) and BCP (6 nm) were evaporated under high vacuum on top of the interlayer. Finally, a 100 nm thick Ag electrode was deposited through a shadow mask. The active area of our device is 0.09 cm^2.

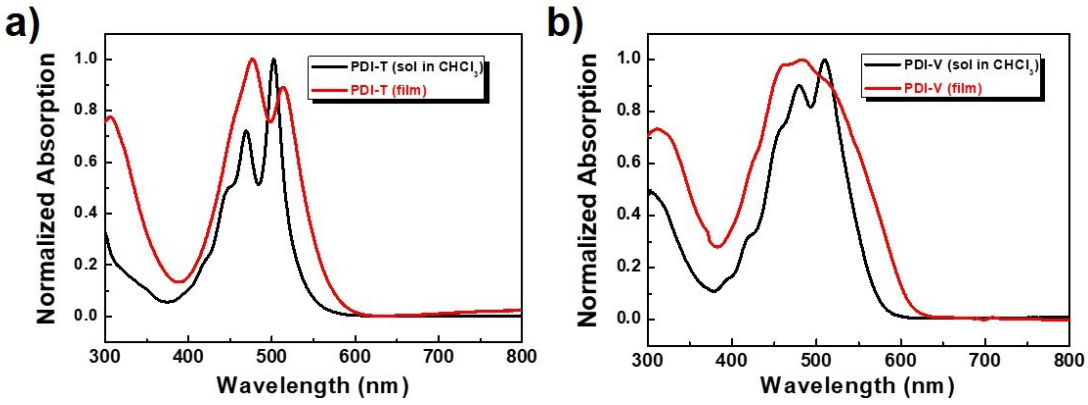

Figure S1. UV-vis absorption spectra of PDI-T a) and PDI-V b) in $CHCl_3$ and in film state, respectively.

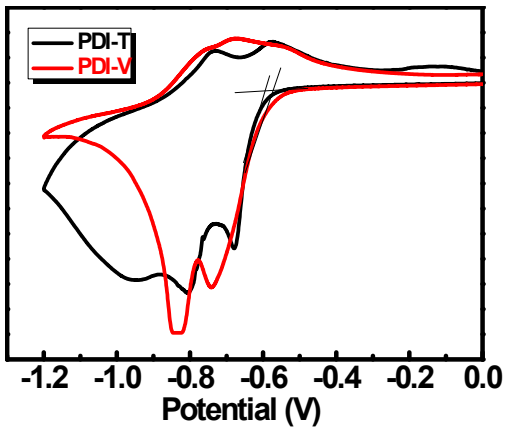

Figure S2. CV measurements of PDI-T and PDI-V.

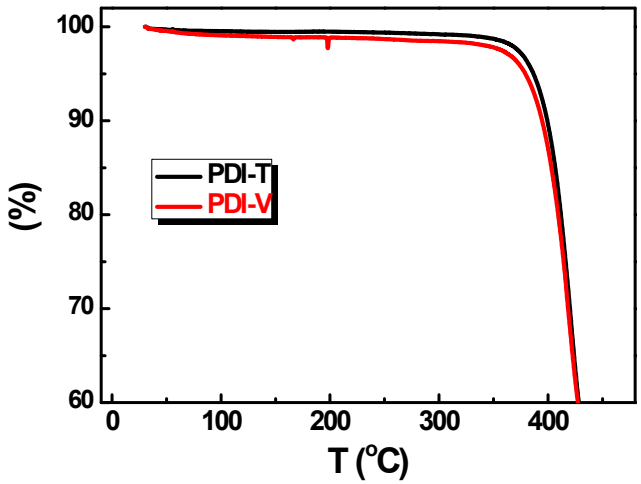

Figure S3. TGA measurements of PDI-T and PDI-V.

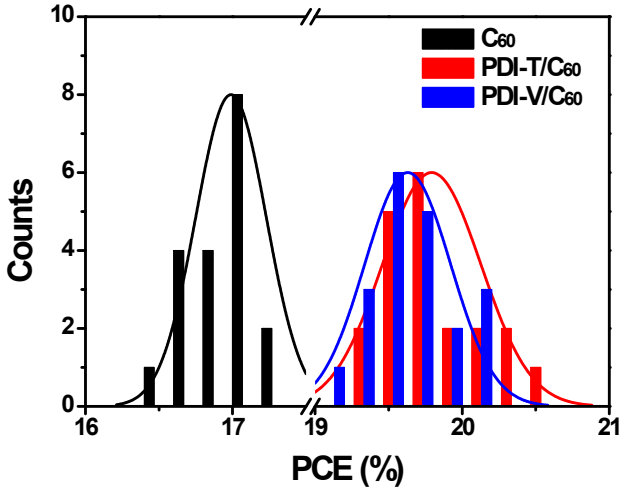

Figure S4. PCE distribution statistics of the control device, and devices with different interlayers.

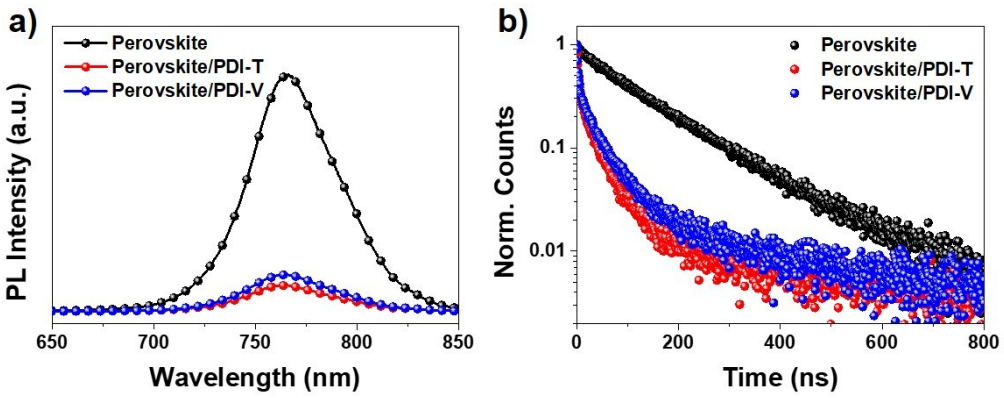

Figure S5. a) Steady-state photoluminescence (PL) and b) time-resolved photoluminescence (TRPL) spectra of perovskite film, and that covered by PDI-T or PDI-V interlayer.

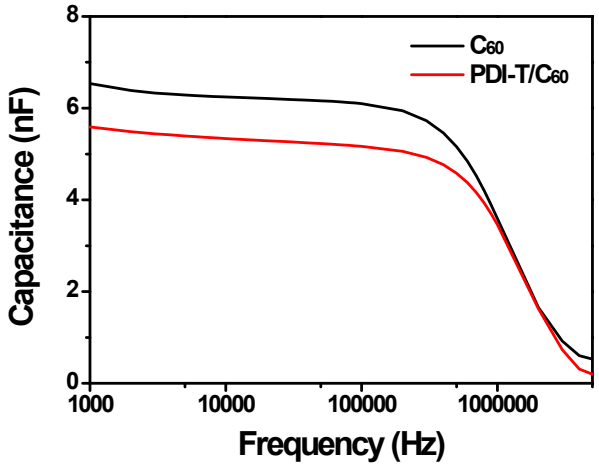

Figure S6. Frequency dependence of the measured capacitance in control device and device with the PDI-T interlayer.

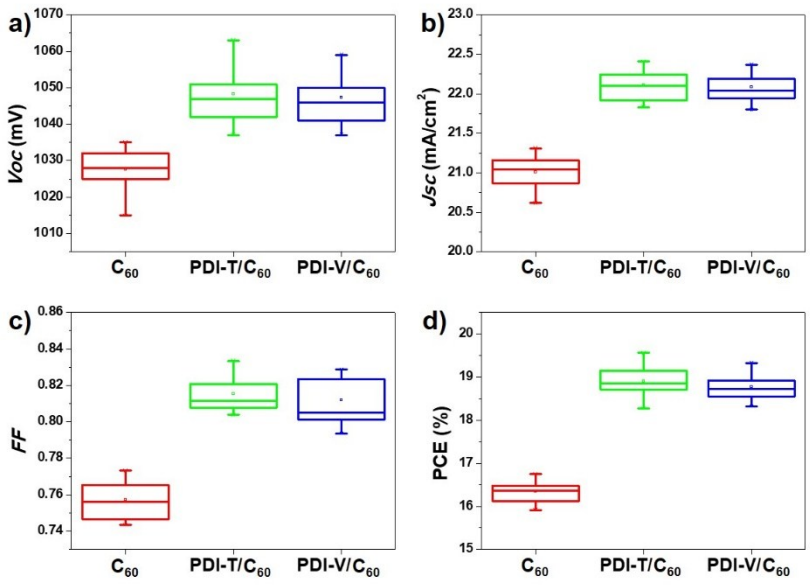

Figure S7. Photovoltaics parameters statistic for the control device, and devices with PDI-T or PDI-V as ETL for inverted PSCs.

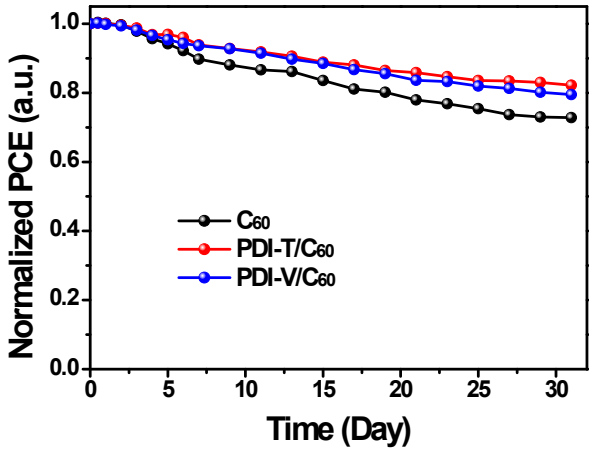

Figure S8. Stability of devices with and without interlayers.

Table S1. Photovoltaic parameters of the inverted devices with PDI-T or PDI-V interfacial material under forward and reverse scan directions, respectively.

Interlayer	Scan direction	V_{OC} (mV)	J_{SC} (mA cm^{-2})	FF	PCE (%)
PDI-T/C_{60}	forward	1086	22.30	82.46	19.97
	reverse	1092	22.35	83.63	20.41

PDI-V/C_{60}	forward	1083	22.20	81.98	19.71
	reverse	1093	22.24	82.98	20.17

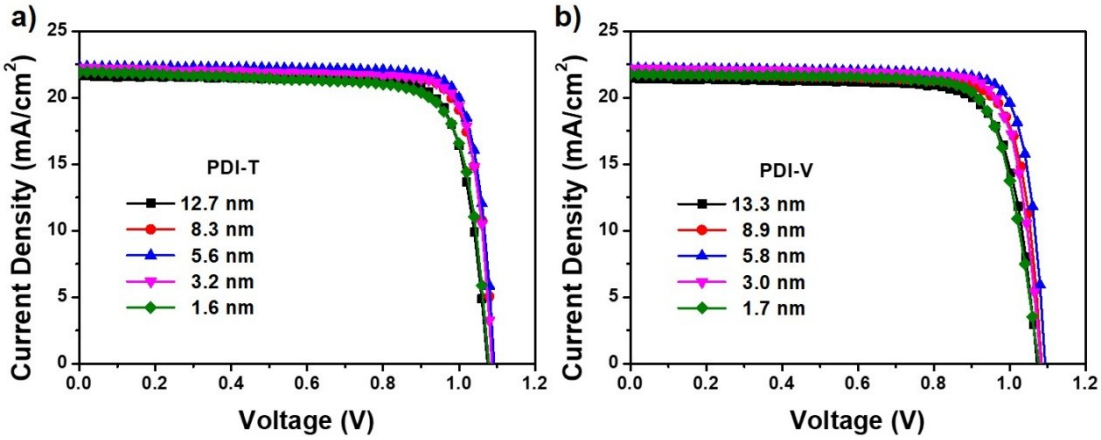

Figure S9. *J-V* curves of PSCs with a) PDI-T interlayer and b) PDI-V interlayer at different thicknesses, respectively.

Table S2. Photovoltaic parameters of the device with PDI-T interlayer in different thicknesses.

PDI-T	V_{OC} (mV)	J_{SC} (mA cm^{-2})	FF	PCE (%)
12.7 nm	1075	21.64	80.69	18.77
8.3 nm	1092	22.17	82.00	19.85
5.6 nm	1092	22.35	83.63	20.41
3.2 nm	1086	22.26	82.48	19.94
1.6 nm	1078	21.95	80.04	18.49

Table S3. Photovoltaic parameters of the device with PDI-V interlayer in different thicknesses.

PDI-V	V_{OC} (mV)	J_{SC} (mA cm^{-2})	FF	PCE (%)
13.3 nm	1072	21.45	78.45	18.04
8.9 nm	1084	21.92	80.47	19.12
5.8 nm	1093	22.24	82.98	20.17
3.0 nm	1082	22.20	81.26	19.52
1.7 nm	1077	21.76	78.51	18.40

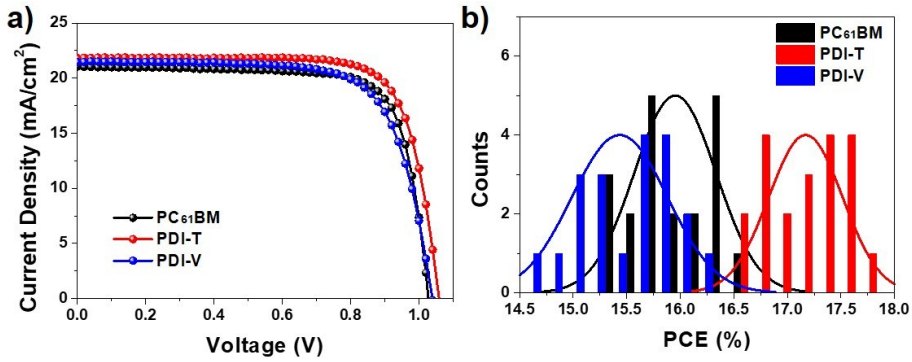

Figure S10. Photovoltaic performances of inverted PSCs using PDI-T/PDI-V as the electron transporting material (ETM).

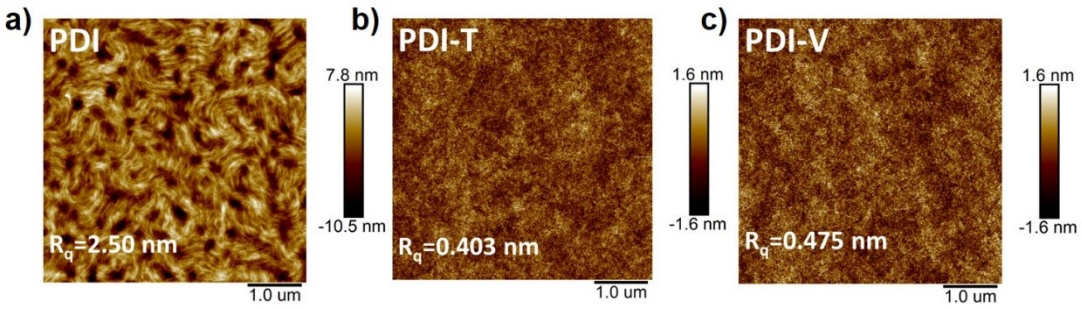

Figure S11. AFM images of a) pristine PDI film, b) PDI-T film and c) PDI-V film.

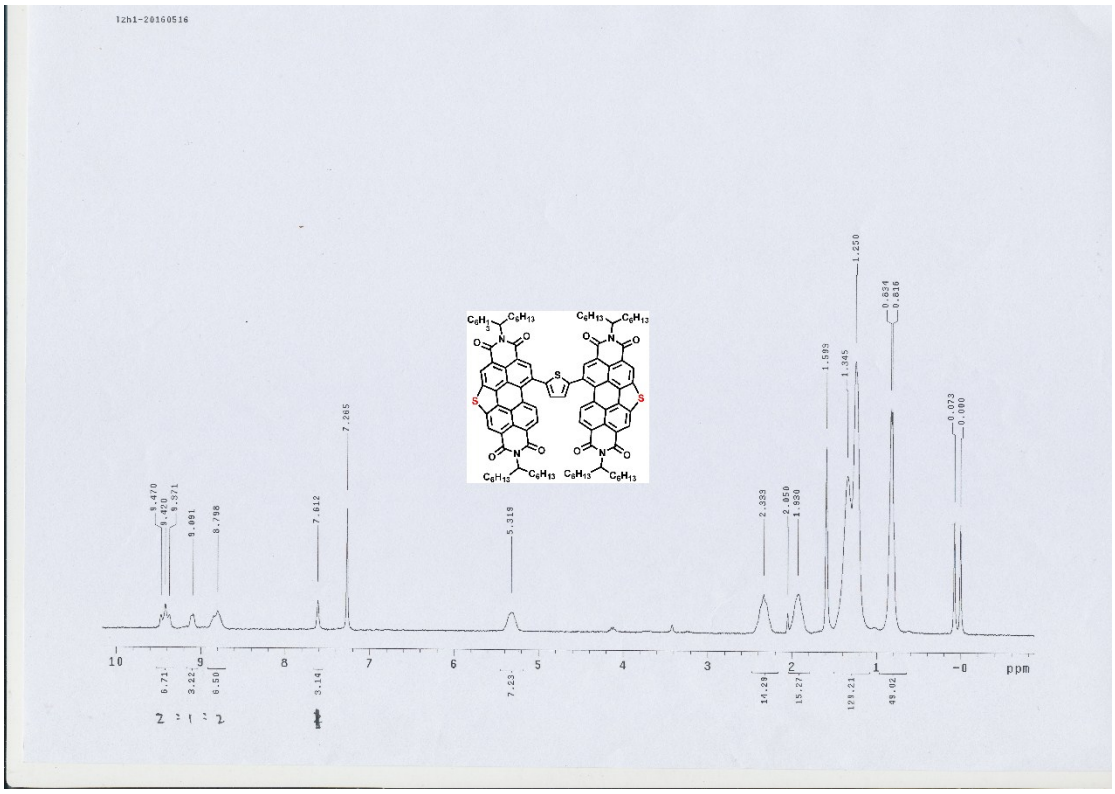

Figure S12. ^{1}H NMR spectrum of PDI-T.

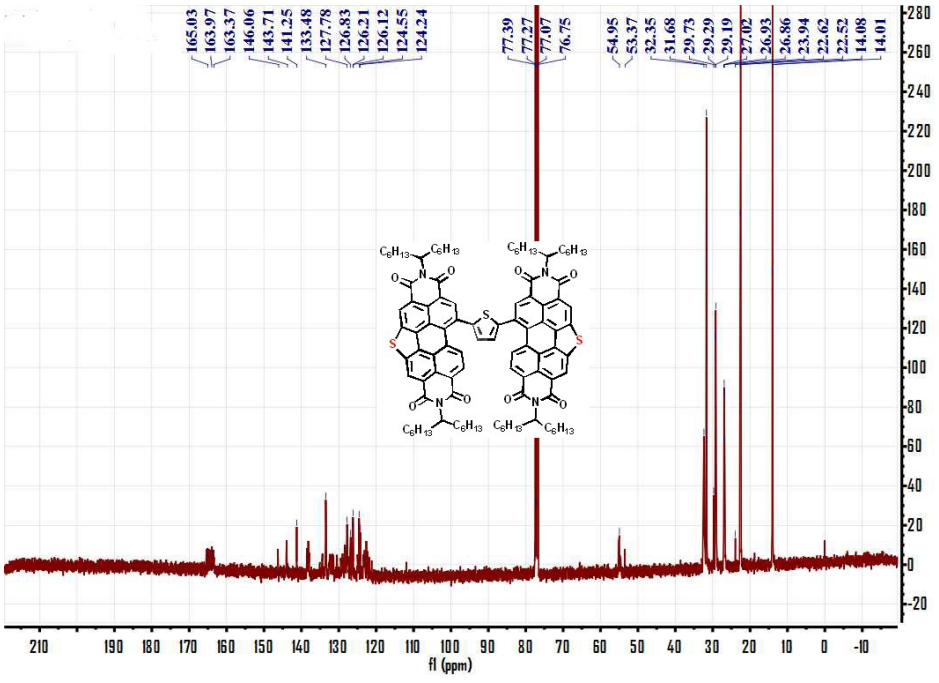

Figure S13. ^{13}C NMR spectrum of PDI-T.

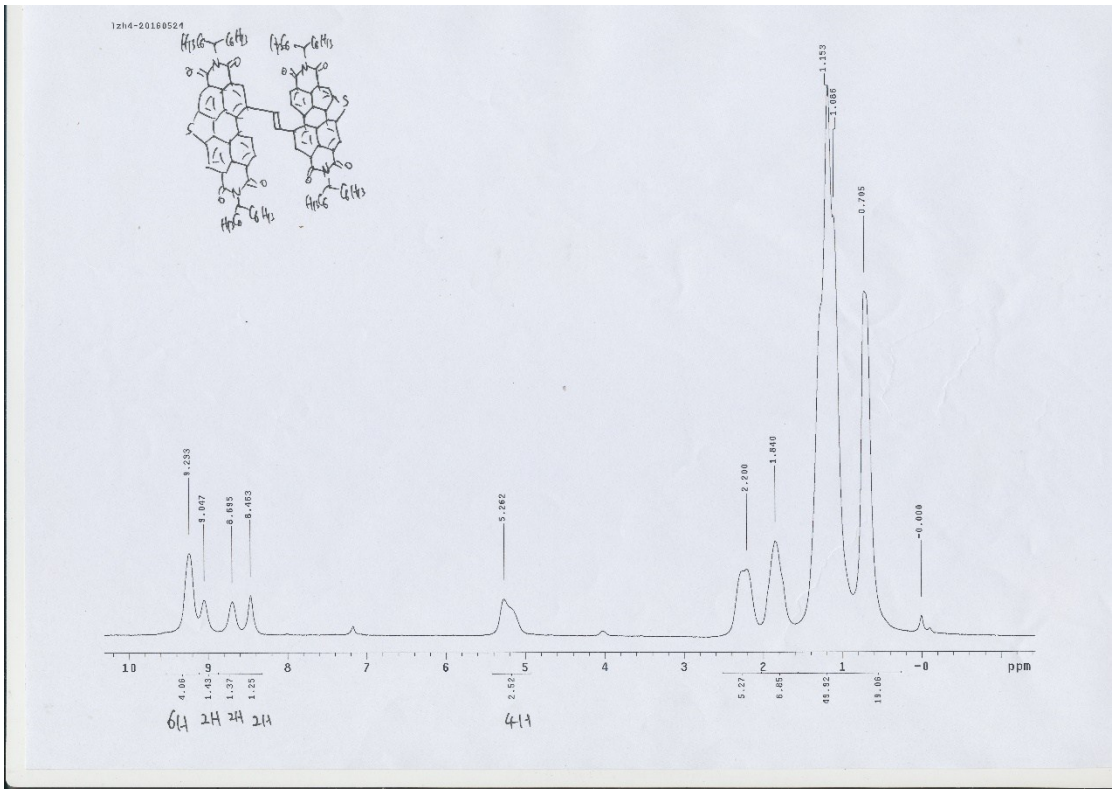

Figure S14. ^{1}H NMR spectrum of PDI-V.

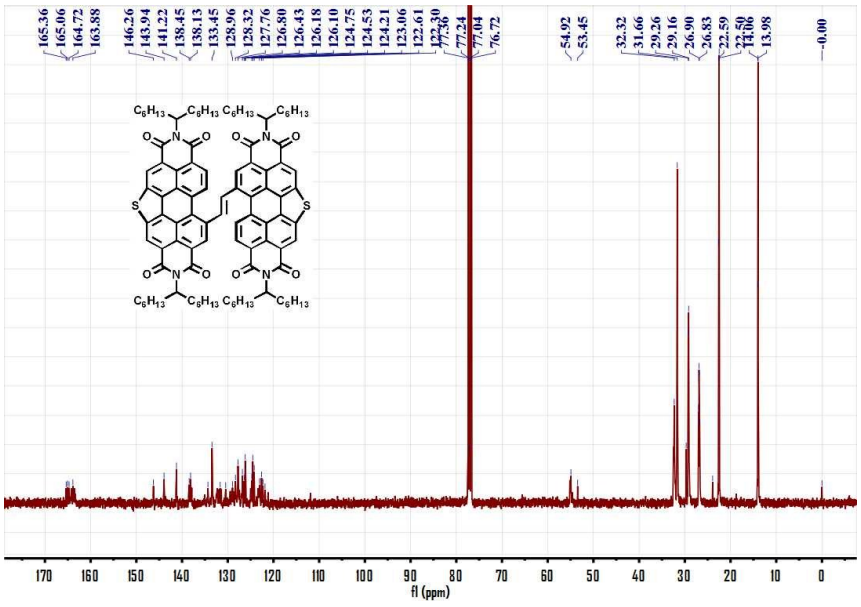

Figure S15. ^{13}C NMR spectrum of PDI-T.

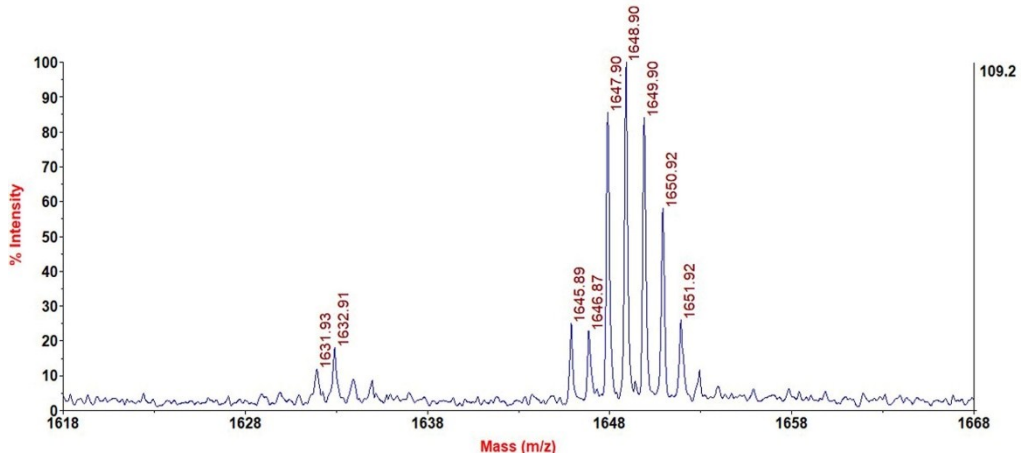

Figure S16. MALDI-TOF spectrum of PDI-T.

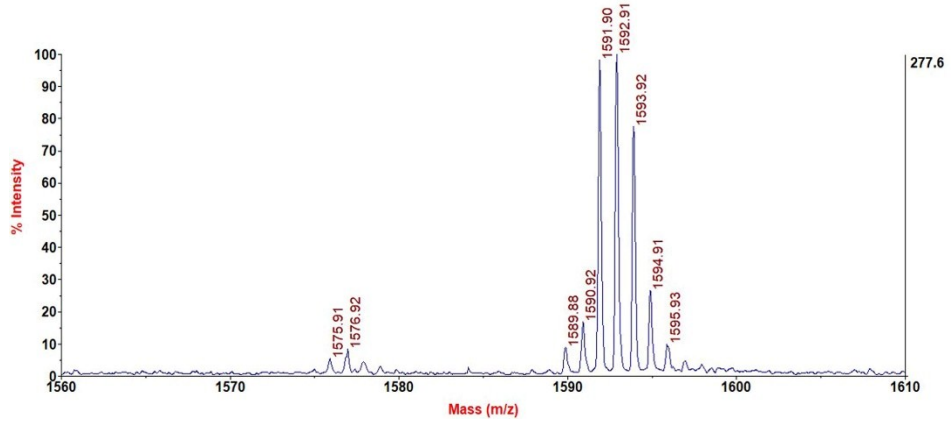

Figure S17. MALDI-TOF spectrum of PDI-V.

References

[1] Z. Luo, W. Xiong, T. Liu, W. Cheng, K. Wu, Y. Sun, C. Yang, *Org. Electron*. **2017**, *41*, 166.

[2] X. Li, X. Liu, X. Wang, L. Zhao, T. Jiu, J. Fang, *J. Mater. Chem. A*. **2015**, *3*, 15024.